Astronomy & Astrophysics manuscript no. 13672
January 13, 2010

The FERRUM project: laboratory-measured transition probabilities for Cr II

J. Gurell[1], H. Nilsson[2], L. Engström[3], H. Lundberg[3], R. Blackwell-Whitehead[2], K. E. Nielsen[4,5], and S. Mannervik[1]

[1] Department of Physics, Stockholm University, AlbaNova University Center, SE-10691 Stockholm, Sweden
e-mail: jonas.gurell@fysik.su.se
[2] Lund Observatory, Lund University, Box 43, SE-22100 Lund, Sweden
[3] Atomic Physics, Department of Physics, Lund University, Box 118, SE-22100 Lund, Sweden
[4] Catholic University of America, Washington, DC 20064, USA
[5] Astrophysics Science Division, Code 667, Goddard Space Flight Center, Greenbelt, MD 20771, USA

Received XXX; accepted XXX

ABSTRACT

Aims. We measure transition probabilities for Cr II transitions from the $z\,^4\mathrm{H}_J$, $z\,^2\mathrm{D}_J$, $y\,^4\mathrm{F}_J$, and $y\,^4\mathrm{G}_J$ levels in the energy range 63000 to 68000 cm^{-1}.
Methods. Radiative lifetimes were measured using time-resolved laser-induced fluorescence from a laser-produced plasma. In addition, branching fractions were determined from intensity-calibrated spectra recorded with a UV Fourier transform spectrometer. The branching fractions and radiative lifetimes were combined to yield accurate transition probabilities and oscillator strengths.
Results. We present laboratory measured transition probabilities for 145 Cr II lines and radiative lifetimes for 14 Cr II levels. The laboratory-measured transition probabilities are compared to the values from semi-empirical calculations and laboratory measurements in the literature.

Key words. Atomic data, Line: identification, Methods: laboratory, Techniques: spectroscopic

1. Introduction

Spectral analysis of astrophysical objects depends on the availability of accurate laboratory data including radiative lifetimes and transition probabilities. Lines of Cr II are observed in a broad range of stellar and nebular spectra (e.g. Merrill 1951; Shevchenko 1994; Andrievsky et al. 1994), and accurate Cr data are required for stellar abundance studies (Babel & Lanz 1992; Dimitrijević et al. 2007). In particular, several chemically peculiar stars show unexpectedly high abundances of Cr (Rice & Wehlau 1994; López-García et al. 2001).

Radiative lifetimes in Cr II have been with the beam-foil technique by Pinnington et al. (1973) and Engman et al. (1975) and with the time-resolved laser-induced fluorescence (TRLIF) technique by Schade et al. (1990), Pinnington et al. (1993), and Nilsson et al. (2006). In addition, branching fraction (BF) measurements were combined with radiative lifetimes to yield transition probabilities (Bergeson & Lawler 1993; Spreger et al. 1994; Gonzalez et al. 1994; Nilsson et al. 2006), and oscillator strengths were measured by Musielok & Wujec (1979), Goly & Weniger (1980) and Wujec & Weniger (1981) using a wall-stabilized arc. Semi-empirical oscillator strengths have been calculated by Kurucz (1988) using the Cowan code, by Luke (1988) using the R matrix method, and by Raasen & Uylings (1997) using the orthogonal operator method.

Several studies have found that the stellar chromium abundance determined from Cr I lines is significantly different to the abundance using Cr II lines (McWilliam et al. 1995;Sobeck et al. 2007;Lai et al. 2008). This difference is greater than the uncertainty in the stellar observations and measured oscillator strengths. Furthermore, the difference increases as the metallicity of the star decreases. Sobeck et al. (2007) indicate that one possible explanation of this discrepancy could be non-LTE effects not included in the stellar model. Sobeck et al. (2007) propose that, in order to resolve this issue additional laboratory investigations of chromium should focus on weak branches of Cr II and that the Cr abundance should be reanalyzed with a three-dimensional hydrodynamical model. In addition, the need for more laboratory measured Cr II transition probabilities is discussed by Wallace & Hinkle (2009).

In this paper we present transition probabilities for 145 lines in Cr II from 14 upper levels, see the partial energy level diagram of Cr II in Figure 1. The lifetimes of the upper levels have been measured with the TRLIF technique.

2. Laboratory measurements

The lifetime of an upper state i can be written as

$$\tau_{\mathrm{i}} = 1/\sum_k A_{\mathrm{ik}}, \tag{1}$$

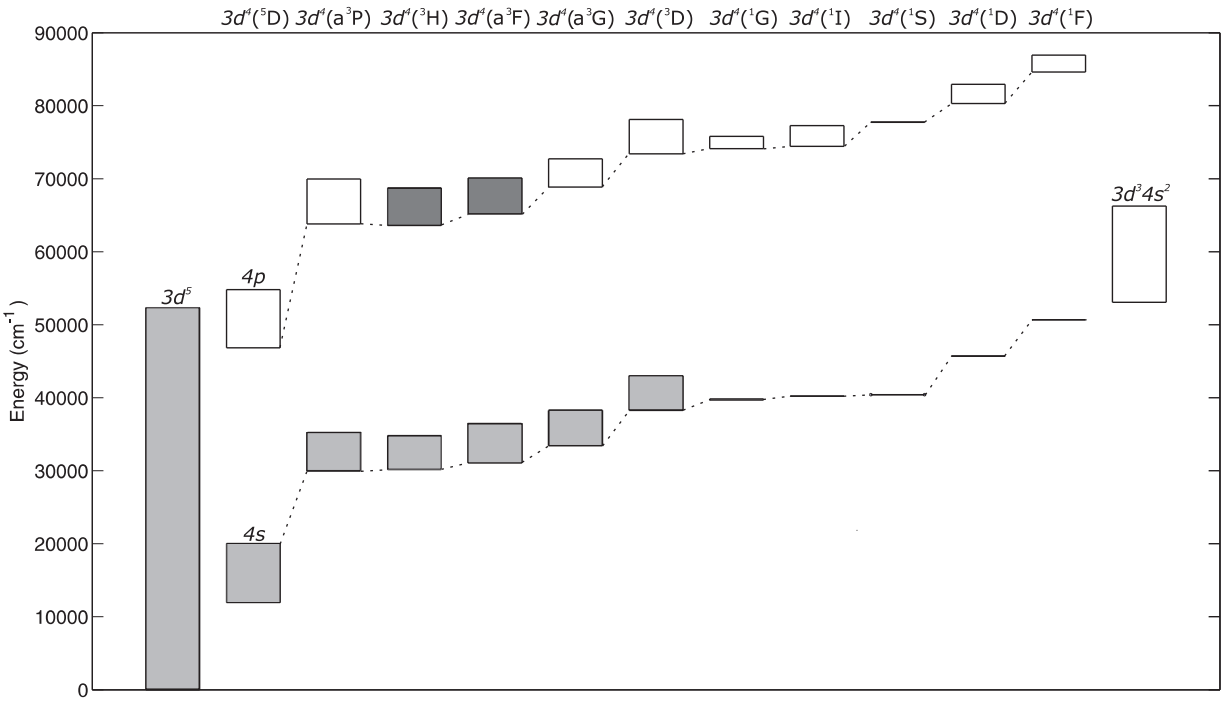

Fig. 1. Partial energy level diagram of Cr II (Ralchenko et al. 2009). Only terms belonging to the $3d^5$, $3d^4 4s$, $3d^4 4p$, and $3d^3 4s^2$ configurations are shown and ordered by their respective parent term shown above the diagram. The investigated upper levels are shown as dark grey boxes and the lower levels to which they decay are shown as light grey boxes.

where A_{ik} is the transition probability of a line from upper level i to lower level k. The BF of the line is defined as

$$BF_{ik} = A_{ik} / \sum_k A_{ik} = I_{ik} / \sum_k I_{ik}, \quad (2)$$

where I_{ik} is the measured intensity corrected for the instrumental response. Combining these two equations gives the transition probabilities as

$$A_{ik} = BF_{ik} / \tau_{\rm i}. \quad (3)$$

The following subsections describe the measurements of the lifetimes and BFs.

2.1. Radiative lifetimes

We measured lifetimes for 14 odd parity levels in Cr II belonging to the $3d^4 4p$ configuration. The lifetimes were measured using the TRLIF technique at the Lund High Power Laser Facility. This technique has been described in detail in the literature (see Bergström et. al. 1988, Xu et al. 2003), so only a brief description is given here.

A laser-produced 'plasma-cone' containing Cr atoms and ions in metastable levels was created by focusing a Nd:YAG laser (Continuum Surelite) onto a target of pure Cr. Cr^+ ions in metastable states were excited to levels of opposite parity using a pump laser and the fluorescence from the excited levels was recorded as a function of time. The excitation pulses were created by pumping a Continuum Nd-60 dye laser with a Nd:YAG Continuum NY-82 laser. The pulses from the Nd:YAG pump laser were shortened from 10 to 1.5 ns using stimulated Brillouin scattering. The Nd-60 dye laser used a DCM dye to produce light between 6000 and 6700 Å. A broader wavelength coverage was achieved by using nonlinear effects in KDP and BBO crystals and Raman shifts in a H_2 cell.

A 1/8 m monochromator was used to select the observable fluorescence wavelength. The fluorescence signal was recorded with a micro-channel plate photomultiplier tube with a rise time of 0.2 ns. The shape of the excitation pulse was measured with the same system as the fluorescence signal. The lifetimes were extracted by fitting the fluorescence data with a single exponential convoluted with the shape of the laser pulse. Each lifetime curve was averaged over 1000 laser shots, and the final lifetimes given in Table 1 are averages of at least 10 lifetime curves. The uncertainties in the lifetimes include both statistical and systematic errors.

2.2. Branching fractions

The BFs were measured from spectra recorded with the Chelsea Instrument FT500 UV FT spectrometer at Lund Observatory. The light source was a Penning discharge lamp with pure Cr cathodes and operated with Ne as buffer gas. The light source was operated at a current between 0.8 and 1.3 A, and with at a carrier gas pressure of 40 mTorr. The Penning discharge lamp provides an intensity stable emission spectrum over several hours enabling high signal-to-noise (S/N) spectra to be recorded. Figure 2 shows part of the observed spectrum.

Three separate spectral regions were recorded to cover the wavenumber region between 20000 and 52000 $\rm cm^{-1}$.

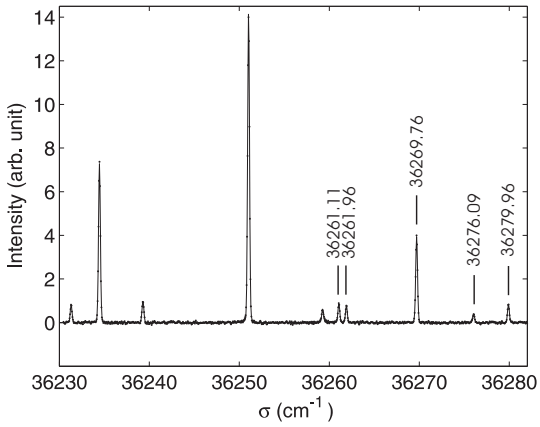

Fig. 2. A section of the FT spectrum showing five Cr II lines indicated by their respective wavenumber.

The spectra were intensity-calibrated with standard lamps with known spectral radiances and by Cr II BFs previously measured by Nilsson et al. (2006). A continuous deuterium (D_2) lamp was used in the wavenumber range $32000 - 52000\,\mathrm{cm}^{-1}$. A tungsten strip lamp was used in the wavenumber range $20000 - 28000\,\mathrm{cm}^{-1}$ and the 28000-32000 cm^{-1} wavenumber region was calibrated using previously intensity-calibrated Cr II BFs from the data of Nilsson et al. (2006). The calibration was performed with a software routine implemented in the program XGremlin (Nave et al. 1997). In addition, the spectra were wavenumber-calibrated using an average of nine unblended Ne II lines, which have been measured with high accuracy and suggested as suitable transitions for wavenumber calibration by Öberg (2007).

However, the wavelengths and wavenumbers in Tables 2 and 3 are Ritz values determined from the energy levels in Ralchenko et al. (2009).

The spectral lines were fitted with Voigt profiles to determine the integrated intensity using the commercially available software PeakFit. The uncertainty in the integrated intensity is determined from the standard deviation in the fitted values and the S/N of the lines. The majority of the fitted Cr II line profiles were unblended. However, a small number of Cr II lines were partially blended with other lines. The blended features were identified, and a fit of both line profiles was performed when possible. The blended Cr II lines are given with larger uncertainties in the integrated intensity.

3. Results

Our experimental lifetimes are compared to previous measurements and calculations in Table 1. Table 2 shows our laboratory measured BFs, A-values and semi-empirical BFs. The complete line list for all Cr II lines measured in this paper with comparisons to semi-empirical log gf values in the literature is shown in Table 3. A comparison between our measured A-values and values presented in the literature is shown in Table 4.

3.1. Lifetimes

In Table 1 we report radiative lifetimes for 14 levels in Cr II compared with values from the literature. Our experimental lifetimes of the $z\,^4$H term agree, within the uncertainties, with the beam-foil measurements by Pinnington et al. (1973) and by Engman et al. (1975), and the experimental lifetimes of Warner (1967). There is a good agreement between our lifetimes and the values from Raasen & Uylings (1997); however, the calculated values by Warner (1967) and Luke (1988) are shorter than our lifetimes by approximately four standard deviations.

There is a a three-sigma difference between our lifetimes for the $y\,^4$G term and the measured values of Pinnington et al. (1973). The difference may come from the improved wavelength resolution of our measurements. Pinnington et al. (1973) were not able to resolve the four individual levels $y\,^4$G and measured an average lifetime determined from a blend of transitions from these levels. Pinnington et al. (1973) also states that the assignment of the transition from the $y\,^4$G term at 2700 Å is one of the 'less certain' ones presented. In our measurements we have resolved the individual decay channels.

There is good agreement between our work and the lifetimes calculated by Raasen & Uylings (1997) for the $y\,^4\mathrm{F}_{9/2,\,7/2}$ levels. However, there is a discrepancy between our lifetimes and the values of Raasen & Uylings (1997) for $y\,^4\mathrm{F}_{5/2,\,3/2}$ and the $z\,^2\mathrm{D}_{5/2,\,3/2}$. This may be due to a difference in the predicted level mixing, which is difficult to reproduce in semi-empirical calculations for complex atomic systems such as Cr II. In addition, an increase in the predicted level mixing may explain the discrepancy between our experimental BFs and the calculated BFs by Raasen & Uylings (1997) for transitions from the $y\,^4\mathrm{F}_{5/2,\,3/2}$ and the $z\,^2\mathrm{D}_{5/2,\,3/2}$ levels.

3.2. Transition probabilities

In Table 2 we present our BFs and A-values. The BF residual value in Table 2 is determined from the semi-empirical calculations of Raasen & Uylings (1997). The residual value is used to estimate the BF contribution from transitions that were not observed in our spectra. The missing lines are very weak transitions, $BF \leq 2\%$, and for most upper levels in Table 2, the residual value is at most a few percent, which is less than the uncertainty in the BFs. The uncertainty in the A-values is determined from the BF and lifetime uncertainty using the method discussed by Sikström et al. (2002), which include uncertainties from the line-fitting, intensity calibration of each spectra, intensity cross calibration between separate spectra and the uncertainty in the fit of the decay curve.

The $a\,^4\mathrm{P}_{3/2}$-$y\,^4\mathrm{F}_{5/2}$ transition at $36704.65\,\mathrm{cm}^{-1}$ and the $a\,^4\mathrm{F}_{9/2}$-$y\,^4\mathrm{G}_{11/2}$ transition at $34514.88\,\mathrm{cm}^{-1}$ were found to be considerably stronger than predicted by semi-empirical calculations. This deviation stems from line blending with other Cr II transitions. The line at $36704.65\,\mathrm{cm}^{-1}$ is within $0.05\,\mathrm{cm}^{-1}$ of a line of comparable strength from the $b\,^4\mathrm{G}_{11/2}$-$y\,^2\mathrm{H}_{11/2}$ transition and the line at $34514.88\,\mathrm{cm}^{-1}$ is within $0.05\,\mathrm{cm}^{-1}$ of the $b\,^2\mathrm{I}_{11/2}$-$z\,^2\mathrm{I}_{13/2}$ transition. We observed other relatively strong transitions from these $y\,^2\mathrm{H}_{11/2}$ and $z^2\mathrm{I}_{13/2}$ upper levels, which indicated that these levels had relatively high populations and were

Table 1. Lifetimes in Cr II

			τ (ns)							
Configuration	Term	E (cm^{-1})	This work	C&B[a]	WT[b]	P[c]	WE[d]	E[e]	L[f]	R&U[g]
$(a\,^3\mathrm{H})4p$	$z\,^4\mathrm{H}^o_{7/2}$	63600	4.4(4)	2.1(4)[h]	3.3[h]	4.0(4)[h]	5.3[h,i]		3.3	4.4
$(a\,^3\mathrm{H})4p$	$z\,^4\mathrm{H}^o_{9/2}$	63706	4.4(4)	2.1(4)[h]	3.3[h]	4.0(4)[h]	5.3[h,i]		3.3	4.4
$(a\,^3\mathrm{H})4p$	$z\,^4\mathrm{H}^o_{11/2}$	63849	4.2(3)	2.1(4)[h]	3.3[h]	4.0(4)[h]	5.3[h,i]	5.0(5)	3.3	4.4
$(a\,^3\mathrm{H})4p$	$z\,^4\mathrm{H}^o_{13/2}$	64031	4.2(3)	2.1(4)[h]	3.3[h]	4.0(4)[h]	5.3[h,i]	4.7(5)	3.3	4.3
$(a\,^3\mathrm{F})4p$	$y\,^4\mathrm{F}^o_{5/2}$	67012	3.7(4)							4.3
$(a\,^3\mathrm{F})4p$	$y\,^4\mathrm{F}^o_{3/2}$	67070	3.9(5)							4.5
$(a\,^3\mathrm{F})4p$	$y\,^4\mathrm{F}^o_{7/2}$	67393	2.9(2)							2.9
$(a\,^3\mathrm{F})4p$	$y\,^4\mathrm{F}^o_{9/2}$	67448	2.9(2)							2.9
$(a\,^3\mathrm{H})4p$	$y\,^4\mathrm{G}^o_{7/2}$	67333	2.6(2)			3.4(2)[h]				2.6
$(a\,^3\mathrm{H})4p$	$y\,^4\mathrm{G}^o_{5/2}$	67344	2.6(2)			3.4(2)[h]				2.5
$(a\,^3\mathrm{H})4p$	$y\,^4\mathrm{G}^o_{9/2}$	67353	2.6(2)			3.4(2)[h]				2.5
$(a\,^3\mathrm{H})4p$	$y\,^4\mathrm{G}^o_{11/2}$	67369	2.7(2)			3.4(2)[h]				2.5
$(a\,^3\mathrm{F})4p$	$z\,^2\mathrm{D}^o_{3/2}$	67379	3.1(3)							3.3
$(a\,^3\mathrm{F})4p$	$z\,^2\mathrm{D}^o_{5/2}$	67387	3.1(3)							3.4

[a] Corliss and Bozman (1962) (Intensity measurement)
[b] Warner (1967) (Calculated)
[c] Pinnington et al.(1973) (Beam-foil measurement)
[d] Warner (1967) (Emission measurement)
[e] Engman (1975) (Beam-foil measurement)
[f] Luke (1988) (Calculated)
[g] Raasen & Uylings (1997) (Calculated)
[h] Mean lifetime
[i] Upper limit

thus probable candidates for line blending. However, it was impossible to fit the two blended features to recover the individual line intensities because of the close proximity of the central wavenumbers of the transitions. Instead we used BFs from the semi-empirical calculations of Raasen & Uylings (1997) for the 36704.65 cm^{-1} and 34514.88 cm^{-1} transitions.

The log gfs in Table 3 are compared to the semi-empirical results by Kurucz (1988) and Raasen & Uylings (1997) and a graphical comparison is given in Figs. 3 and 4. The comparison between our laboratory log gfs and those of Raasen & Uylings (1997), Figure 4, has a smaller deviation than those in Figure 3.

There is good agreement between our experimental log gf values and the semi-empirical log gf values of Kurucz (1988) for lines from the $z\,^4\mathrm{H}_J$ levels as well as for lines from the $y\,^4\mathrm{G}_{5/2}$ and the $z\,^2\mathrm{D}_{3/2}$ levels, see Table 3. However, there is a larger deviation between our log gf values and the semi-empirical calculations of Kurucz (1988) for lines from the $y\,^4\mathrm{F}_J$ levels, the $y\,^4\mathrm{G}_{7/2,9/2,11/2}$ levels, and the $z\,^2\mathrm{D}_{5/2}$ level. This may be due to inaccurate level mixing in the semi-empirical calculations of Kurucz (1988). The semi-empirical calculations of Raasen & Uylings (1997) agree more consistently with our laboratory log gf values.

In Table 4 we compare our A-values with A-values in the literature. In general our A-values agree to within the uncertainties with the results in the literature; however, the A-values of Corliss & Bozman (1962) are significantly different to the other A-values in the literature. The compilation of Corliss & Bozman (1962) includes many values determined from a wall-stabilized arc. Inaccuracies in the wall temperature measurement for the wall-stabilized arc method can significantly increase the uncertainty in the measurement, so we recommend that the A-values in Corliss & Bozman (1962) are used with caution.

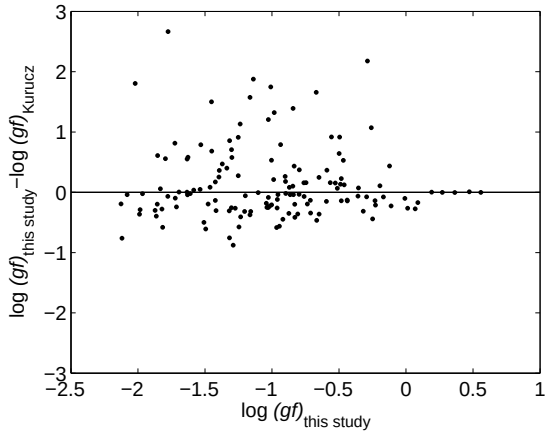

Fig. 3. Comparison between log (gf)-values from this experimental study and semi-empirical values from Kurucz (1988). The difference between the two values for each line is plotted as a function of line strength.

4. Summary

We present experimental lifetimes for 14 highly excited energy levels in Cr II and BFs for 145 transitions from these levels, yielding experimental transition probabilities for

Table 4. A comparison between our A-values and the A-values in the literature.

Upper level	Lower level	σ (cm^{-1})	$A(10^8\,s^{-1})$ This study	R&U[a]	K[b]	W&W[c]	G&W[d]	M[e]	Wt[f]	We[g]	C&B[h]
$3d^4(^3H)4p\ ^4H^o_{13/2}$	$3d^4(^3G)4s\ ^4G_{11/2}$	30336.36	0.099	0.207	0.318			0.33	0.17	0.17[i]	0.86
$3d^4(^3H)4p\ ^4H^o_{13/2}$	$3d^4(^3H)4s\ ^4H_{13/2}$	33638.67	1.951	1.787	2.003			2.0	1.5	1.5[i]	5.1
$3d^4(^3H)4p\ ^4H^o_{11/2}$	$3d^4(^3H)4s\ ^4H_{11/2}$	33550.22	1.851	1.672	1.804			1.9	1.6	1.7[i]	5.1
$3d^4(^3H)4p\ ^4H^o_{9/2}$	$3d^4(^3H)4s\ ^4H_{9/2}$	33487.47	1.720	1.600	2.207			2.3	1.7	1.8[i]	3.6
$3d^4(^3H)4p\ ^4H^o_{7/2}$	$3d^4(^3H)4s\ ^4H_{7/2}$	33444.12	1.741	1.602	2.186			2.3	0.52	0.55[i]	6.1
$3d^4(^3H)4p\ ^4G^o_{9/2}$	$3d^4(^3H)4s\ ^4H_{9/2}$	37134.48	0.100	0.186	0.183		0.13(7)				
$3d^4(^3F)4p\ ^4F^o_{5/2}$	$3d^4(^1D)4s\ ^2D_{5/2}$	21281.50	0.011	0.006	0.007	0.046(9)			0.0492		

[a] Raasen & Uylings (1997)
[b] Kurucz (1988)
[c] Wujec and Weniger (1981)
[d] Goly and Weniger (1980)
[e] Musielok (1975)
[f] Warner (1967) (Calculated)
[g] Warner (1967) (Experimental)
[h] Corliss and Bozman (1962)
[i] Upper limit

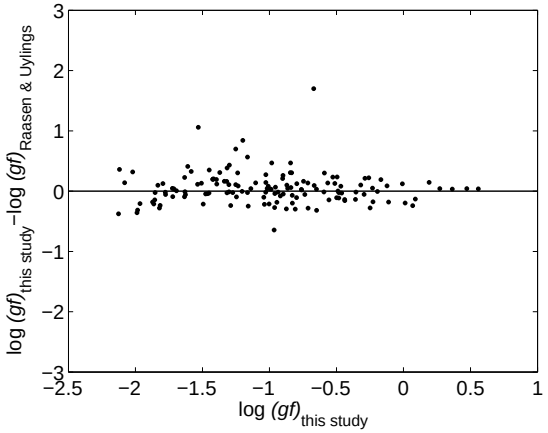

Fig. 4. Comparison between $\log(gf)$-values from this experimental study and semi-empirical values from Raasen & Uylings (1997). The difference between the two values for each line is plotted as a function of line strength.

lines that are strong features in stellar spectra. For the majority of the Cr II transitions in this paper, the experimental transition probabilities agree with the semi-empirical calculations within the uncertainty of the measurements. In particular, we note that the semi-empirical orthogonal operator calculations of Raasen & Uylings (1997) have a one standard deviation difference to our experimental log gf values of 0.21. However, the semi-empirical Cowan code calculations of Kurucz (1988) have a one standard deviation difference to our experimental log gf values of 0.61. In addition, different semi-empirical calculations produce different term labels for the energy levels because of the large amount of level mixing. We suggested that further theoretical calculations for Cr II would benefit studies of this ion.

Acknowledgements. JG and SM are very grateful for the warm hospitality shown by the staff at Lund Observatory. Financial support from the Swedish Research Council (VR), a Linnaeus grant to the Lund Laser Centre and the Knut and Alice Wallenberg Foundation, is gratefully acknowledged. RBW acknowledges a Euopean Commision Marie Curie Intra-European fellowship.

References

Andrievsky, S. M., Kovtyukh, V. V. & Usenko, A. 1994, A&A, 281, 465
Babel, J. &Lanz, T. 1992, A&A, 263, 232
Bergeson, S. D. & Lawler, J. E. 1993, ApJ, 408, 382
Bergström, H., Faris, H., Hallstadius, G. W., Lundberg, H., Persson, A. & Wahlström, C. G. 1988, Z. Phys. D 8, 17
Corliss, C. H. & Bozman, W. R. 1962, Nat. Bur. Std. Monograph, 53
Dimitrijević, M. S., Ryabchikova, T., Simić, Popović, Ľ. C. & Dačić M. 2007, A&A, 469, 681
Engman, B., Gaupp, A., Curtis, L. J. & Martinsson, I. 1975, Phys. Scr., 12, 220
Goly, A. & Weniger, S. 1980, J. Quant. Spectrosc. Radiat. Transfer, 24, 335
Gonzalez, A. M., Ortiz, M. & Campos, J. 1994, Can. J. Phys., 72, 57
Kurucz, R. L. 1988, Trans. IAU, XXB, M. McNally, ed., (Dordrecht: Kluwer), 168
Lai, D. K., Bolte, M., Johnson, J. A., Lucatello, S., Heger, A. & Woosley, S. E. 2008, ApJ, 681, 1524
López-García, Z., Adelman, Saul J. & Pintado, O. I. 2001, A&A, 367, 859
Luke, T. M. 1988, J. Phys. B, 21, 4049
McWilliam, A., Preston, G. W., Sneden, C. & Searle, L. 1995, AJ, 109, 2757
Merrill, P. W. 1951, ApJ, 114, 37
Musielok, J. & Wujec, T. 1979, A&A Suppl., 38, 119
Nave, G., Sansonetti, C. J. & Griesmann, U. 1997, Optical Society of America Technical Digest, 3, 38
Nilsson, H., Ljung, G., Lundberg, H. & Nielsen, K. E. 2006, A&A, 445, 1165
Pinnington, E. H., Lutz, H. O. & Carriaveao, G. W. 1973, Nucl. instrum. Methods, 110, 55
Pinnington, E. H. et al. 1993, Can. J. Phys., 71, 470
Raasen, A. J. J. & Uylings, P. H. M. 1997, unpublished data available at: `ftp://ftp.wins.uva.nl/pub/orth/chromium`
Ralchenko, Yu., Kramida, A.E., Reader, J., and NIST ASD Team (2009). NIST Atomic Spectra Database (version 3.1.5), [Online]. Available: http://physics.nist.gov/asd3 [2009, October 12]. National Institute of Standards and Technology, Gaithersburg, MD.
Rice, J. B. & Wehlau, W. H. 1994, A&A, 291, 825
Schade, W., Mundt, B. & Helbig, V. 1990, Phys. Rev. A, 42, 3
Shevchenko, V. S. 1994, Astron. Zh., 71, 572
Sikström, C. M., Nilsson, H., Litzén, U., Blom, A. & Lundberg, H. 2002, J. Quant. Spectrosc. Radiat. Transfer, 74, 355
Sobeck, J. S., Lawler, J. E. & Sneden, C. 2007, ApJ, 667, 1267
Spreger, R., Schelm, B., Kock, M., Neger, T. & Ulbel, M. 1994, J. Quant. Spectrosc. Radiat. Transfer, 51, 779
Wallace, L. & Hinkle, K. 2009, ApJ, 700, 720
Warner, B. 1967, Memoirs Roy. Astron. Soc., 70, 165

Wujec, T. & Weniger, S. 1981, J. Quant. Spectrosc. Radiat. Transfer, 25, 167
Xu, H. L., Svanberg, S., Quinet, P., Garnir, H. P., and Biémont É 2003, J. Phys. B: At. Mol. Opt. Phys. 36 4773
Öberg, K. J. 2007, Eur. Phys. J. D, 41, 25

Table 2. Observed transitions, experimental BFs and A-values presented along with calculated BFs using the orthogonal operator approach (Raasen & Uylings 1997)

Upper level	Lower level	σ (cm^{-1})	λ_{air} (Å)	BF Exp.	BF Theory [a]	A ($10^7\,s^{-1}$)	Unc (%)
$3d^4(^3H)4p\ ^4H^o_{13/2}$	$3d^4(^3H)4s\ ^2H_{11/2}$	29217.60	3421.613	0.002	0.004	0.06	20
	$3d^4(^3G)4s\ ^4G_{11/2}$	30336.36	3295.425	0.042	0.089	0.99	14
	$3d^4(^3H)4s\ ^4H_{13/2}$	33638.67	2971.902	0.819	0.771	19.50	7
	$3d^5\ ^2I_{13/2}$	33880.64	2950.679	0.007	0.001	0.16	32
	$3d^5\ ^4G_{11/2}$	43518.41	2297.171	0.125	0.135	2.97	14
	Residual			0.002			
$3d^4(^3H)4p\ ^4H^o_{11/2}$	$3d^4(^3H)4s\ ^2H_{9/2}$	29217.80	3421.591	0.002	0.001	0.04	76
	$3d^4(^3G)4s\ ^4G_{11/2}$	30154.56	3315.294	0.002	0.005	0.05	14
	$3d^4(^3G)4s\ ^4G_{9/2}$	30229.75	3307.047	0.041	0.083	0.99	14
	$3d^5\ ^4F_{9/2}$	30994.42	3225.456	0.002	0.004	0.04	16
	$3d^4(^3F)4s\ ^4F_{9/2}$	32629.36	3063.834	0.011	0.008	0.27	14
	$3d^4(^3H)4s\ ^4H_{13/2}$	33456.86	2988.052	0.038	0.034	0.90	14
	$3d^4(^3H)4s\ ^4H_{11/2}$	33550.22	2979.737	0.780	0.736	18.56	7
	$3d^5\ ^4G_{9/2}$	43329.42	2307.191	0.112	0.120	2.66	14
	$3d^5\ ^4G_{11/2}$	43336.59	2306.809	0.009	0.009	0.21	16
	Residual			0.004			
$3d^4(^3H)4p\ ^4H^o_{9/2}$	$3d^4(^3G)4s\ ^4G_{9/2}$	30087.32	3322.704	0.004	0.008	0.09	18
	$3d^4(^3G)4s\ ^4G_{7/2}$	30185.16	3311.933	0.042	0.083	0.95	15
	$3d^5\ ^4F_{7/2}$	30869.55	3238.504	0.003	0.005	0.07	20
	$3d^4(^3F)4s\ ^4F_{7/2}$	32537.67	3072.469	0.013	0.010	0.29	17
	$3d^4(^3H)4s\ ^4H_{11/2}$	33407.78	2992.442	0.057	0.054	1.29	15
	$3d^4(^3H)4s\ ^4H_{9/2}$	33487.47	2985.321	0.761	0.704	17.29	9
	$3d^5\ ^4G_{9/2}$	43186.97	2314.802	0.013	0.013	0.29	16
	$3d^5\ ^4G_{7/2}$	43188.45	2314.722	0.101	0.116	2.28	15
	Residual			0.008			
$3d^4(^3H)4p\ ^4H^o_{7/2}$	$3d^5\ ^2G_{9/2}$	27328.36	3658.160	0.014	0.000	0.33	15
	$3d^4(^3G)4s\ ^4G_{7/2}$	30079.75	3323.539	0.003	0.008	0.08	22
	$3d^4(^3G)4s\ ^4G_{5/2}$	30182.87	3312.184	0.045	0.088	1.02	15
	$3d^4(^3F)4s\ ^4F_{5/2}$	32483.54	3077.588	0.009	0.005	0.20	20
	$3d^4(^3H)4s\ ^4H_{9/2}$	33382.07	2994.747	0.056	0.051	1.27	15
	$3d^4(^3H)4s\ ^4H_{7/2}$	33444.12	2989.190	0.766	0.709	17.40	9
	$3d^5\ ^4G_{7/2}$	43083.05	2320.386	0.011	0.012	0.26	17
	$3d^5\ ^4G_{5/2}$	43088.79	2320.077	0.101	0.118	2.29	15
	Residual			0.009			
$3d^4(a\ ^3F)4p\ ^4F^o_{3/2}$	$3d^4(^1S)4s\ ^2S_{1/2}$	26655.36	3750.525	0.009	0.009	0.22	16
	$3d^5\ ^2F_{5/2}$	27328.42	3658.160	0.031	0.005	0.79	12
	$3d^4(^3F)4s\ ^2F_{5/2}$	31501.25	3173.559	0.031	0.038	0.80	17
	$3d^4(^3P)4s\ ^2P_{3/2}$	31714.54	3152.215	0.493	0.464	12.63	8
	$3d^4(^3P)4s\ ^2P_{1/2}$	32411.20	3084.458	0.067	0.065	1.72	12
	$3d^5\ ^2D_{5/2}$	35719.56	2798.762	0.105	0.136	2.70	11
	$3d^4(^3F)4s\ ^4F_{5/2}$	35953.09	2780.581	0.028	0.036	0.72	15
	$3d^4(^3F)4s\ ^4F_{3/2}$	35987.56	2777.920	0.027	0.051	0.69	14
	$3d^4(^3P)4s\ ^4P_{5/2}$	36205.99	2761.157	0.014	0.019	0.37	22
	$3d^5\ ^4P_{1/2}$	45246.70	2209.417	0.021	0.019	0.55	18
	$3d^5\ ^4P_{5/2}$	45247.91	2209.358	0.020	0.018	0.50	19
	$3d^5\ ^4G_{5/2}$	46558.37	2147.165	0.068	0.054	1.73	13
	Residual			0.087			
$3d^4(a\ ^3F)4p\ ^4F^o_{5/2}$	$3d^4(^1D)4s\ ^2D_{5/2}$	21281.50	4697.602	0.005	0.003	0.13	30
	$3d^4(^3D)4s\ ^2D_{5/2}$	24114.12	4145.780	0.029	0.022	0.77	12
	$3d^5\ ^2F_{7/2}$	27135.04	3684.223	0.041	0.025	1.12	12

Table 2. continued.

Upper level	Lower level	σ (cm^{-1})	λ_{air} (Å)	BF Exp.	BF Theory[a]	A ($10^7\,s^{-1}$)	Unc (%)
	$3d^5\ ^2F_{5/2}$	27270.08	3665.979	0.062	0.002	1.69	12
	$3d^4(^1G)4s\ ^2G_{7/2}$	27328.36	3658.160	0.031	0.012	0.82	12
	$3d^4(^3F)4s\ ^2F_{7/2}$	31404.56	3183.330	0.042	0.221	1.13	12
	$3d^4(^3F)4s\ ^2F_{5/2}$	31442.88	3179.450	0.003	0.020	0.08	17
	$3d^4(^3P)4s\ ^2P_{3/2}$	31656.18	3158.027	0.101	0.061	2.73	12
	$3d^4(^3G)4s\ ^4G_{7/2}$	33491.04	2985.002	0.008	0.013	0.23	67
	$3d^5\ ^2F_{5/2}$	34408.71	2905.390	0.018	0.013	0.47	39
	$3d^5\ ^2D_{5/2}$	35661.19	2803.343	0.097	0.005	2.61	12
	$3d^4(^3F)4s\ ^4F_{7/2}$	35843.49	2789.084	0.029	0.043	0.77	14
	$3d^4(^3F)4s\ ^4F_{5/2}$	35894.74	2785.102	0.032	0.038	0.85	15
	$3d^4(^3F)4s\ ^4F_{3/2}$	35929.18	2782.432	0.027	0.034	0.73	15
	$3d^4(^3P)4s\ ^4P_{5/2}$	36147.63	2765.616	0.175	0.172	4.72	12
	$3d^4(^3P)4s\ ^4P_{3/2}$	36704.65	2723.644	0.024[1]	0.024	0.53	12
	$3d^5\ ^4D_{7/2}$	41978.40	2381.451	0.010	0.012	0.26	59
	$3d^5\ ^4P_{3/2}$	45187.88	2212.293	0.008	0.004	0.21	28
	$3d^5\ ^4P_{5/2}$	45189.56	2212.211	0.034	0.020	0.92	18
	$3d^5\ ^4G_{7/2}$	46494.27	2150.126	0.118	0.081	3.19	12
	$3d^4(^5D)4s\ ^6D_{7/2}$	46988.03	2127.530	0.042	0.021	1.13	22
	Residual			0.072			
$3d^4(a\ ^3F)4p\ ^4F^o_{7/2}$	$3d^4(^3G)4s\ ^4G_{9/2}$	33774.50	2959.949	0.027	0.024	0.94	13
	$3d^4(^3G)4s\ ^4G_{7/2}$	33872.35	2951.398	0.020	0.018	0.69	16
	$3d^5\ ^4F_{7/2}$	34556.79	2892.939	0.100	0.105	3.45	10
	$3d^4(^3F)4s\ ^4F_{9/2}$	36174.11	2763.592	0.047	0.073	1.62	10
	$3d^4(^3F)4s\ ^4F_{7/2}$	36224.86	2759.719	0.188	0.275	6.48	9
	$3d^4(^3F)4s\ ^4F_{5/2}$	36276.09	2755.822	0.016	0.028	0.56	13
	$3d^4(^3P)4s\ ^4P_{5/2}$	36528.98	2736.743	0.004	0.007	0.15	32
	$3d^4(^3H)4s\ ^4H_{9/2}$	37174.66	2689.206	0.093	0.127	3.20	10
	$3d^4(^3H)4s\ ^4H_{7/2}$	37236.70	2684.726	0.008	0.009	0.27	16
	$3d^5\ ^4D_{5/2}$	42346.73	2360.736	0.005	0.007	0.16	22
	$3d^5\ ^4G_{9/2}$	46874.16	2132.698	0.115	0.091	3.95	10
	$3d^5\ ^4G_{7/2}$	46875.64	2132.631	0.274	0.165	9.45	8
	$3d^4(^5D)4s\ ^6D_{5/2}$	47595.59	2100.368	0.069	0.037	2.38	13
	Residual			0.034			
$3d^4(a\ ^3F)4p\ ^4F^o_{9/2}$	$3d^4(^3D)4s\ ^4D_{7/2}$	29179.00	3426.140	0.002	0.003	0.07	22
	$3d^4(^3H)4s\ ^2H_{11/2}$	32635.58	3063.250	0.006	0.005	0.19	26
	$3d^4(^3G)4s\ ^4G_{9/2}$	33829.60	2955.127	0.010	0.011	0.36	24
	$3d^5\ ^4F_{9/2}$	34594.28	2889.804	0.139	0.150	4.79	10
	$3d^4(^3F)4s\ ^4F_{9/2}$	36229.20	2759.389	0.292	0.419	10.07	9
	$3d^4(^3F)4s\ ^4F_{7/2}$	36279.96	2755.528	0.027	0.044	0.94	11
	$3d^4(^3H)4s\ ^4H_{11/2}$	37150.07	2690.986	0.029	0.032	1.00	11
	$3d^5\ ^4G_{9/2}$	46929.24	2130.195	0.118	0.064	4.08	14
	$3d^5\ ^4G_{11/2}$	46936.43	2129.869	0.271	0.187	9.35	9
	$3d^4(^5D)4s\ ^6D_{7/2}$	47424.51	2107.946	0.073	0.053	2.53	12
	Residual			0.032			
$3d^4(a\ ^3H)4p\ ^4G^o_{5/2}$	$3d^4(^3G)4s\ ^4G_{5/2}$	33926.02	2946.729	0.036	0.038	1.39	31
	$3d^5\ ^4F_{3/2}$	34499.28	2897.762	0.094	0.067	3.60	12
	$3d^4(^3F)4s\ ^4F_{3/2}$	36261.11	2756.960	0.061	0.044	2.34	11
	$3d^4(^3H)4s\ ^4H_{7/2}$	37187.26	2688.294	0.310	0.452	11.92	10
	$3d^5\ ^4G_{7/2}$	46826.20	2134.883	0.093	0.045	3.57	12
	$3d^5\ ^4G_{5/2}$	46831.93	2134.622	0.373	0.321	14.34	9
	Residual			0.034			

[1] Based on theoretical A-value from Ref.[1]

Table 2. continued.

Upper level	Lower level	σ (cm^{-1})	λ_{air} (Å)	BF Exp.	BF Theory[a]	A ($10^7\,s^{-1}$)	Unc (%)
$3d^4$(a ^{3}H)$4p$ $^4G^o_{7/2}$	$3d^4(^1D)4s$ $^2D_{5/2}$	21603.17	4627.654	0.005	0.000	0.21	23
	$3d^4(^3G)4s$ $^4G_{7/2}$	33812.68	2956.607	0.017	0.018	0.65	17
	$3d^5$ $^4F_{5/2}$	34478.83	2899.480	0.084	0.083	3.22	12
	$3d^5$ $^4F_{7/2}$	34497.16	2897.940	0.010	0.006	0.38	31
	$3d^5$ $^2F_{5/2}$	34730.42	2878.476	0.025	0.013	0.94	28
	$3d^5$ $^2D_{5/2}$	35982.90	2778.278	0.007	0.008	0.25	44
	$3d^4(^3F)4s$ $^4F_{9/2}$	36114.43	2768.159	0.014	0.014	0.55	15
	$3d^4(^3F)4s$ $^4F_{7/2}$	36165.19	2764.273	0.038	0.030	1.47	11
	$3d^4(^3F)4s$ $^4F_{5/2}$	36216.44	2760.361	0.090	0.114	3.46	10
	$3d^4(^3H)4s$ $^4H_{9/2}$	37114.99	2693.530	0.168	0.317	6.47	10
	$3d^4(^3H)4s$ $^4H_{7/2}$	37177.03	2689.035	0.021	0.036	0.80	12
	$3d^5$ $^4G_{9/2}$	46814.49	2135.417	0.262	0.156	10.06	9
	$3d^5$ $^4G_{7/2}$	46816.06	2135.345	0.228	0.179	8.76	9
	$3d^5$ $^4G_{5/2}$	46821.68	2135.089	0.024	0.018	0.91	19
	Residual			0.009			
$3d^4$(a ^{3}H)$4p$ $^4G^o_{9/2}$	$3d^4(^3G)4s$ $^4G_{9/2}$	33734.32	2963.474	0.019	0.019	0.71	22
	$3d^5$ $^4F_{7/2}$	34516.61	2896.307	0.091	0.091	3.51	11
	$3d^4(^3F)4s$ $^4F_{7/2}$	36184.69	2762.784	0.075	0.094	2.87	11
	$3d^4(^3H)4s$ $^4H_{11/2}$	37054.78	2697.907	0.245	0.374	9.42	10
	$3d^4(^3H)4s$ $^4H_{9/2}$	37134.48	2692.116	0.026	0.047	1.00	11
	$3d^5$ $^4G_{9/2}$	46833.98	2134.528	0.373	0.270	14.36	9
	$3d^5$ $^4G_{7/2}$	46835.47	2134.460	0.036	0.025	1.38	13
	$3d^5$ $^4G_{11/2}$	46841.16	2134.201	0.122	0.068	4.68	11
	Residual			0.014			
$3d^4$(a ^{3}H)$4p$ $^4G^o_{11/2}$	$3d^4(^3H)4s$ $^2H_{9/2}$	32738.14	3053.653	0.009	0.004	0.34	19
	$3d^4(^3G)4s$ $^4G_{11/2}$	33674.95	2968.700	0.019	0.015	0.70	26
	$3d^5$ $^4F_{9/2}$	34514.88	2896.452	0.096[2]	0.096	3.56	11
	$3d^4(^3F)4s$ $^4F_{9/2}$	36149.73	2765.456	0.071	0.097	2.64	12
	$3d^4(^3H)4s$ $^4H_{13/2}$	36977.23	2703.565	0.239	0.389	8.85	11
	$3d^4(^3H)4s$ $^4H_{11/2}$	37070.59	2696.756	0.020	0.032	0.75	12
	$3d^5$ $^2I_{13/2}$	37219.20	2685.988	0.005	0.002	0.19	14
	$3d^5$ $^4G_{9/2}$	46849.77	2133.809	0.026	0.016	0.96	20
	$3d^5$ $^4G_{11/2}$	46856.96	2133.482	0.508	0.343	18.83	11
	Residual			0.006			
$3d^4$(a ^{3}F)$4p$ $^2D^o_{3/2}$	$3d^4(^3D)4s$ $^2D_{3/2}$	24392.68	4098.434	0.006	0.006	0.19	27
	$3d^5$ $^2F_{5/2}$	27637.24	3617.274	0.015	0.010	0.48	17
	$3d^4(^3F)4s$ $^2F_{5/2}$	31810.11	3142.745	0.050	0.049	1.62	13
	$3d^4(^3P)4s$ $^2P_{3/2}$	32023.39	3121.812	0.055	0.054	1.76	13
	$3d^5$ $^4F_{5/2}$	34524.32	2895.660	0.021	0.025	0.69	21
	$3d^5$ $^4F_{3/2}$	34534.58	2894.800	0.107	0.107	3.44	13
	$3d^4(^3F)4s$ $^4F_{5/2}$	36261.96	2756.896	0.062	0.083	1.99	13
	$3d^4(^3F)4s$ $^4F_{3/2}$	36296.41	2754.280	0.248	0.366	7.99	12
	$3d^5$ $^4G_{5/2}$	46867.22	2133.015	0.337	0.215	10.87	11
	$3d^4(^5D)4s$ $^6D_{1/2}$	47851.04	2089.154	0.048	0.033	1.53	33
	Residual			0.052			
$3d^4$(a ^{3}F)$4p$ $^2D^o_{5/2}$	$3d^4(^3D)4s$ $^2D_{5/2}$	24489.14	4082.291	0.003	0.006	0.10	32
	$3d^5$ $^2F_{7/2}$	27510.06	3633.998	0.008	0.007	0.26	21
	$3d^4(^3F)4s$ $^2F_{7/2}$	31779.58	3145.763	0.042	0.055	1.35	13
	$3d^4(^3P)4s$ $^2P_{3/2}$	32031.19	3121.052	0.021	0.028	0.67	17
	$3d^4(^3G)4s$ $^4G_{7/2}$	33865.99	2951.953	0.022	0.019	0.71	20
	$3d^5$ $^4F_{5/2}$	34532.14	2895.004	0.092	0.094	2.98	12

[2] Based on theoretical A-value from Ref.[1]

Table 2. continued.

Upper level	Lower level	σ (cm^{-1})	λ_{air} (Å)	BF Exp.	BF Theory[a]	A ($10^7\,s^{-1}$)	Unc (%)
	$3d^5\ ^2F_{5/2}$	34783.80	2874.058	0.029	0.008	0.92	17
	$3d^4(^3F)4s\ ^4F_{7/2}$	36218.51	2760.204	0.072	0.099	2.32	12
	$3d^4(^3F)4s\ ^4F_{5/2}$	36269.76	2756.303	0.199	0.298	6.42	11
	$3d^4(^3F)4s\ ^4F_{3/2}$	36304.20	2753.688	0.042	0.075	1.34	13
	$3d^4(^3H)4s\ ^4H_{7/2}$	37230.35	2685.183	0.017	0.008	0.55	15
	$3d^5\ ^4G_{7/2}$	46869.29	2132.920	0.233	0.186	7.51	11
	$3d^5\ ^4G_{5/2}$	46875.02	2132.659	0.109	0.041	3.50	13
	$3d^4(^5D)4s\ ^6D_{3/2}$	47755.83	2093.320	0.044	0.010	1.42	21
	Residual			0.068			

[a]Raasen & Uylings (1997)
[b]Based on theoretical A-value from Raasen & Uylings (1997)

Table 3. Line list and experimental log (gf)-values together with calculated values from the literature.

λ_{vac}	σ	E_{lower}	log gf		
(Å)	(cm^{-1})	(cm^{-1})	This study	K[a]	R&U[b]
2089.819	47851.04	11961.81	−1.396	−1.649	−1.59
2093.985	47755.83	12032.58	−1.252	−1.527	−1.95
2101.035	47595.59	12147.82	−0.899	−1.078	−1.16
2108.614	47424.51	12303.86	−0.746	−0.906	−0.91
2128.202	46988.03	12303.86	−1.316	−2.172	−1.70
2129.869	46936.43	20512.10	−0.169	−0.091	−0.36
2130.195	46929.24	20519.33	−2.277	−0.556	−0.82
2133.304	46875.64	20517.83	−0.288	−2.465	−0.50
2133.332	46875.02	20512.06	−0.843	−2.234	−1.31
2133.372	46874.16	20519.33	−0.666	−0.201	−0.76
2133.593	46869.29	20517.83	−0.512	−0.577	−0.64
2133.687	46867.22	20512.06	−0.528	−0.682	−0.76
2134.155	46856.96	20512.10	+0.188	+0.190	+0.05
2134.482	46849.77	20519.33	−1.105	−1.097	−1.24
2134.875	46841.16	20512.10	−0.495	−1.410	−0.73
2135.134	46835.47	20517.83	−1.027	−0.942	−1.17
2135.202	46833.98	20519.33	−0.008	+0.094	−0.13
2135.295	46831.93	20512.06	−0.231	−0.091	−0.28
2135.557	46826.20	20517.83	−0.835	−1.268	−1.14
2135.763	46821.68	20512.06	−1.303	−1.047	−1.41
2136.019	46816.06	20517.83	−0.319	−0.005	−0.42
2136.091	46814.49	20519.33	−0.259	−1.329	−0.48
2147.841	46558.37	20512.06	−1.319	−1.010	−1.48
2150.126	46494.28	20517.83	−0.713	−0.877	−1.10
2210.047	45247.91	21822.52	−1.833	−1.890	−1.93
2210.106	45246.70	21823.84	−1.795	−2.353	−1.92
2212.900	45189.56	21822.52	−1.371	−1.840	−1.68
2212.983	45187.88	21824.11	−2.021	−3.826	−2.34
2297.879	43518.40	20512.10	−0.483	−0.341	−0.46
2307.519	43336.59	20512.10	−1.694	−1.697	−1.70
2307.901	43329.42	20519.33	−0.594	−0.443	−0.58
2315.434	43188.45	20517.83	−0.736	−0.540	−0.68
2315.513	43186.97	20519.33	−1.630	−1.589	−1.62
2320.789	43088.79	20512.06	−0.830	−0.631	−0.76
2321.099	43083.05	20517.83	−1.777	−1.709	−1.76
2382.178	41978.40	25033.70	−1.853	−2.462	−1.83
2685.523	37236.70	30156.79	−1.627	−2.209	−1.57
2685.981	37230.35	30156.79	−1.450	−2.133	−1.80
2686.785	37219.20	30149.83	−1.612	−1.588	−2.02
2689.093	37187.26	30156.79	−0.111	+0.115	+0.07
2689.833	37177.03	30156.79	−1.159	−0.841	−0.91
2690.004	37174.66	30218.81	−0.556	−1.473	−0.41
2691.785	37150.07	30298.51	−0.936	−1.726	−0.92
2692.915	37134.48	30218.81	−0.962	−0.701	−0.69
2694.329	37114.99	30218.81	−0.249	+0.193	+0.03
2697.556	37070.59	30298.51	−1.005	−0.795	−0.79
2698.707	37054.78	30298.51	+0.012	+0.276	+0.21
2704.367	36977.23	30391.83	+0.066	+0.344	+0.31
2724.450	36704.65	30307.44	−1.451[3]	−2.952	−1.42
2737.552	36528.98	30864.46	−1.872	−1.572	−1.69
2754.502	36304.20	31082.94	−1.038	−0.787	−0.82
2755.093	36296.41	31082.94	−0.439	−0.310	−0.30
2756.343	36279.96	31168.58	−0.945	−0.382	−0.76
2756.637	36276.09	31117.39	−1.289	−0.412	−1.05
2757.118	36269.76	31117.39	−0.358	−0.295	−0.22
2757.711	36261.96	31117.39	−1.042	−0.859	−0.94
2757.775	36261.11	31082.94	−0.796	−1.168	−0.92
2760.204	36229.20	31219.35	+0.088	+0.260	+0.22

[3] Unresolved blend with the line $70398.87_{11/2}$-$33694.15_{11/2}$

Table 3. continued.

λ_{vac}	σ	E_{lower}	log gf		
(Å)	(cm^{-1})	(cm^{-1})	This study	K[a]	R&U[b]
2760.534	36224.87	31168.58	−0.228	−0.015	−0.05
2761.019	36218.51	31168.58	−0.798	−0.765	−0.69
2761.177	36216.44	31117.39	−0.499	−1.141	−0.39
2761.973	36205.00	30864.46	−1.775	−4.440	−1.72
2763.600	36184.69	31168.58	−0.483	−0.710	−0.37
2764.408	36174.11	31219.35	−0.829	−0.414	−0.63
2765.090	36165.19	31168.58	−0.870	−0.951	−0.97
2766.272	36149.73	31219.35	−0.440	−0.294	−0.28
2766.433	36147.63	30864.46	−0.468	−0.997	−0.55
2768.976	36114.43	31219.35	−1.299	−1.876	−1.73
2778.740	35987.53	31082.94	−1.494	−0.886	−1.28
2779.098	35982.90	31350.90	−1.634	−1.635	−1.54
2781.401	35953.10	31117.39	−1.476	−1.280	−1.43
2783.253	35929.18	31082.94	−1.274	−1.010	−1.25
2785.923	35894.74	31117.39	−1.204	−0.885	−1.20
2789.907	35843.49	31168.58	−1.246	−0.670	−1.15
2799.587	35719.56	31350.90	−0.897	−0.877	−0.85
2804.169	35661.19	31350.90	−0.714	−0.581	−0.85
2874.902	34783.80	32603.40	−1.164	−2.739	−1.73
2879.320	34730.42	32603.40	−1.027	−2.233	−1.30
2890.651	34594.28	32854.31	−0.195	−0.302	−0.19
2893.787	34556.79	32836.68	−0.461	−0.585	−0.43
2895.648	34534.58	32844.76	−0.762	−0.920	−0.79
2895.853	34532.14	32854.95	−0.649	−0.895	−0.68
2896.509	34524.32	32854.95	−1.462	−1.546	−1.42
2897.156	34516.61	32836.68	−0.355	−0.427	−0.34
2897.301	34514.88	32854.31	−0.270[4]	−0.219	−0.24
2898.611	34499.28	32844.76	−0.565	−0.724	−0.70
2898.789	34497.16	32836.68	−1.417	−1.112	−1.62
2900.330	34478.83	32854.95	−0.489	−0.623	−0.49
2906.241	34408.71	32603.40	−1.423	−1.594	−1.62
2947.590	33926.02	33417.99	−0.960	−0.841	−0.92
2951.541	33880.61	30149.83	−1.531	−2.319	−2.59
2952.260	33872.35	33521.11	−1.139	−3.016	−1.18
2952.815	33865.99	33521.11	−1.252	−2.163	−1.36
2955.992	33829.60	33618.94	−1.302	−2.009	−1.29
2957.470	33812.68	33521.11	−1.164	−0.790	−1.14
2960.814	33774.50	33618.94	−1.004	−1.535	−1.05
2964.340	33734.32	33618.94	−1.028	−0.776	−1.01
2969.566	33674.95	33694.15	−0.958	−0.918	−1.02
2972.769	33638.67	30391.83	+0.558	+0.559	+0.52
2980.606	33550.22	30298.51	+0.472	+0.465	+0.43
2985.873	33491.04	33521.11	−1.722	−1.625	−1.63
2986.192	33487.47	30218.81	+0.364	+0.368	+0.33
2988.923	33456.86	30391.83	−0.840	−0.800	−0.90
2990.062	33444.12	30156.79	+0.271	+0.273	+0.23
2993.315	33407.78	30298.51	−0.760	−0.690	−0.78
2995.620	33382.07	30218.81	−0.864	−0.825	−0.91
3054.541	32738.14	34630.95	−1.240	−2.370	−1.54
3064.422	32635.58	34812.95	−1.536	−1.584	−1.65
3064.725	32629.36	31219.35	−1.337	−1.737	−1.50
3073.361	32537.67	31168.58	−1.393	−1.756	−1.51
3078.483	32483.54	31117.39	−1.633	−2.185	−1.86
3085.354	32411.20	34659.32	−1.009	−2.756	−1.09
3121.957	32031.19	35355.89	−1.234	−0.827	−1.32
3122.717	32023.39	35355.89	−0.988	−1.198	−1.02
3143.655	31810.11	35569.20	−1.017	−0.789	−1.06
3146.675	31779.58	35607.50	−0.919	−0.471	−0.84

[4] Unresolved blend with the line $74743.28_{13/2}$-$40228.33_{11/2}$

Table 3. continued.

λ_{vac}	σ	E_{lower}	log gf		
(Å)	(cm^{-1})	(cm^{-1})	This study	K[a]	R&U[b]
3153.128	31714.54	35355.89	−0.123	−0.559	−0.21
3158.941	31656.18	35355.89	−0.590	−0.956	−0.89
3174.477	31501.25	35569.20	−1.317	−0.561	−1.29
3180.370	31442.88	35569.20	−2.119	−1.357	−2.48
3184.251	31404.56	35607.50	−0.965	−0.380	−0.32
3226.387	30994.42	32854.31	−2.126	−1.933	−1.75
3239.439	30869.55	32836.68	−1.966	−1.942	−1.76
3296.375	30336.36	33694.15	−0.648	−0.285	−0.33
3307.999	30229.75	33618.94	−0.712	−0.368	−0.43
3312.887	30185.16	33521.11	−0.808	−0.447	−0.51
3313.137	30182.87	33417.99	−0.874	−0.523	−0.58
3316.248	30154.56	33694.15	−1.984	−1.695	−1.67
3323.660	30087.32	33618.94	−1.821	−1.542	−1.54
3324.495	30079.75	33521.11	−1.988	−1.624	−1.63
3422.572	29217.80	34630.95	−2.081	−2.041	−2.22
3422.595	29217.60	34812.95	−1.863	−1.467	−1.65
3427.122	29179.00	38269.59	−1.856	−1.658	−1.71
3618.306	27637.24	32603.40	−1.423	−1.288	−1.62
3635.034	27510.06	32355.68	−1.508	−1.008	−1.64
3659.202	27328.36	36272.54	−1.199[c]	−4.526	−4.54
3659.202	27328.36	32603.40	−1.199[c]	−1.142	−2.04
3659.202	27328.36	39683.75	−1.199[c]	−2.305	−1.45
3667.023	27270.08	32603.40	−0.670	−2.327	−2.37
3685.271	27135.04	32355.68	−0.844	−0.946	−1.15
3751.591	26655.36	40415.09	−1.724	−2.537	−1.77
4083.443	24489.14	42897.99	−1.816	−1.234	−1.58
4099.591	24392.68	42986.62	−1.713	−1.470	−1.75
4146.948	24114.12	42897.99	−0.902	−1.164	−1.11
4628.950	21603.17	45730.58	−1.269	−4.682	−4.74
4698.916	21281.50	45730.58	−1.584	−1.619	−1.91

[a] Kurucz (1988)
[b] Raasen & Uylings (1997)
[c] Use of the theoretical values are encouraged due to line blending.